Preparations for Thrust Measurement and Error Discussion of the IMPULSE Resonant Microwave Cavity

IEPC-2017-254 /ISTS-2017-b-254

Presented at 35th International Electric Propulsion Conference,
Atlanta, Georgia
October 8 – 12, 2017

Michael S. McDonald[1], Michael W. Nurnberger[2] and Logan T. Williams[3]
U. S. Naval Research Laboratory, Washington, D.C., 20375, United States of America

This paper reports on preparations for independent validation and verification (IV&V) of a recently proposed speculative class of spacecraft propulsion which we label an "impulse drive". The most prominent example device, and the only one offering peer-reviewed experimental results, is the closed resonant microwave cavity of White et. al. from NASA Johnson Space Center. White reports anomalous thrust production with no conventional expulsion of reaction mass via a new and unconventional interpretation of physics. Such a device would have remarkable applications for spacecraft propulsion, but the positive experimental results to date, while suggestive, are near the limits of state of the art measurement resolution and subject to significant confounding errors due to thermal drifts and other subtle effects. Our objective is to rigorously weed out potential false positive thrust signals with null and control experiments, create an impartial baseline dataset to either validate or refute claims of anomalous thrust, and if merited form a solid foundation for further experimental and theoretical investigation. We duplicate the resonant geometry (length, diameter, taper) of White's experimental apparatus in a replica cavity with mechanical construction and driving microwave circuit of our own design, with careful attention to maximizing driving RF power capability and cavity resonant quality factor Q. We report on the fabrication and initial thermal testing of our replica cavity and the development of a noncontact RF power interface we dub a "finger joint" to permit frictionless power transmission to a freely swinging torsional thrust stand arm. No thrust measurements have been completed to date; this paper only presents experimental methods and risk reduction test results in preparation for performance measurements on a torsional thrust stand at vacuum. Potential sources of error including thermal drift, RF effects, magnetic tearing via dipole coupling, and electrostrictive response in the cavity dielectric insert are discussed.

I.Introduction

IMPULSE, for the In-Depth Measurement of Performance in Unconventional Low-thrust Spacecraft Engines, is an effort underway at the Naval Research Laboratory to independently validate or refute recent reports of anomalous force (thrust) generated from a closed microwave resonant cavity. The measured thrusting force is anomalous because there is no apparent reaction mass expelled by the device, so as advertised the device either violates the conservation of momentum or is demonstrating some form of new physics to preserve momentum conservation. In most cases this class of device is named by its investigator according to their preferred physical theory. Such names include the Q-thruster or quantum vacuum plasma thruster (QVPT) claimed by White to produce thrust by pushing off the quantum vacuum as a medium[1]; the EMDrive, claimed by Shawyer to work via purely electromagnetic phenomena[2]; and Mach effect thrusters, claimed by Fearn and Woodward to work by varying the inertial mass of a device in phase with a (typically piezoelectric) oscillation[3]. For the time being the authors of this work are agnostic on the physical mechanism at play in these thrusters, if indeed any is present aside from experimental error, and we refer to the whole class as *impulse drives*.

[1] Aerospace Engineer, Propulsion Section, Naval Center for Space Technology, michael.mcdonald@nrl.navy.mil
[2] RF Engineer, Active RF Systems Section, Naval Center for Space Technology
[3] Aerospace Engineer, Propulsion Section, Naval Center for Space Technology

This experimental effort focuses on the cavity point design of White et. al from NASA JSC in Ref. [1] as both the best-described and only peer-reviewed result currently available, and reproduces their cavity geometry while re-engineering the fabrication technique and microwave (RF) power feed system into the cavity. White et. al. observed thrust levels in vacuum of approximately 90 μN force for about 80 W input power with a cavity quality factor Q of about 8000. Our NASA-replica cavity has a Q of about 16000 and we plan to test it under vacuum on a torsional thrust stand with an approximately 5 μN noise floor at power levels up to 100 W in the near term. Assuming that thrust scales linearly with power and at least positively with cavity Q, this leads to an expected thrust signal in the low hundreds of microNewtons assuming the phenomena can be replicated in NRL's facilities.

The following sections discuss the overarching design drivers of our experimental approach, walk through the prospective error sources we anticipate, review our experimental equipment, and present results from basic risk reduction testing performed to date to measure thermal profiles, closed loop frequency feedback control, and the performance of our noncontacting finger joint for frictionless RF power transmission onto the thrust stand.

II.Experiment Design Drivers: Maximizing Signal, Minimizing Noise, and Mitigating or Quantifying Error

Performing a high-fidelity measurement for this class of resonant microwave cavity requires accurate measurement of reported forces of 10s-100s μN at RF powers of order 100 W at about 2 GHz at vacuum. We define "accurate" to be a measurement resolution and/or noise floor of order single microNewtons, in order to eventually permit decomposition of the 10-100 μN total force signals into individual error sources, and/or to distinguish small changes in total signal magnitude due to changes in device under test (DUT) operating conditions such as forward RF power or resonant mode. A typical displacement sensitivity of our torsional thrust stand is of order 1 micron (μm) displacement per 15-20 microNewtons (μN) applied force, given our spring stiffness and 20 cm moment arm. However, at typical operating temperatures our DUT thermally expands by hundreds of microns, so thermal displacements alone could dwarf any true force signal. This makes an impulse drive test fundamentally a signal to noise problem, so improving the signal to noise ratio (SNR) by increasing the force signal and decreasing errors and noise drives our design. To maximize signal we wish to maximize cavity RF power and achieve a good cavity quality factor Q. To minimize noise we wish to minimize DUT heating, minimize thermal drift due to heating that does occur, isolate the stand from vibration, operate stably on resonance indefinitely, and operate at vacuum.

Maximizing RF power delivery to a thrust stand in vacuum typically forces a choice between two bad options. The first is to keep the power amplifier at atmosphere, running high power cables to the thrust stand and accepting the stiffness and thermal expansion from the hot cables corrupting the thrust measurement. Many RF-based plasma propulsion tests have used the former approach.[6], [7] The second is to send only DC power to the thrust stand and perform DC-RF power conversion and RF power amplification on the torsional arm in a self-contained system, accepting the attendant waste heat and mass; White et. al. used this technique.[1] In either case, it is not trivial to decouple thermal and propulsive effects. Shortcomings of on-the-stand amplification method are the limited selection and high cost of vacuum-compatible RF amplifiers and the operating temperature limits of those units. These factors have prevented steady state operating tests of proposed impulse drives in vacuum testing to date.

Here we adopt a new technique to transmit RF power across a wideband noncontact joint, using capacitive coupling between interlaced "fingers" in a stripline-like configuration to transmit up to several hundred watts of power at desired frequencies between 0.7 – 2.5 GHz. This design, discussed in more detail in Section IV-E, permits use of standard rack-mount amplifiers and other equipment and mostly decouples the RF transmission lines from affecting the cavity on the thrust stand.

To minimize DUT heating we use a high-emissivity coating to increase radiative heat transfer, while to minimize thermal drift we use resistive heaters on the cavity external surface to pre-heat the cavity to a stable temperature close to that expected from RF heating before switching over to RF power to take force measurements. While not perfect, this technique reduces the magnitude of the temperature transients associated with RF power cycling. A solid state relay mounted on the thrust stand shorts the resistive heaters during RF testing so that constant current is maintained through the heater wires crossing the torsional pivot bearing at all times, minimizing thermal drift from heater wire expansion.

Finally, to maintain the cavity on resonance we use a simple dither technique implemented in LabView to monitor and adjust the driving frequency to minimize reflected power. While increasing cavity resonant quality factor Q has been reported to increase the anomalous force (see [2] Fig. 1) it also makes it more difficult to keep the cavity on resonance under manual control. The thermal load from Ohmic heating by RF-induced cavity wall currents drives thermal expansion in the cavity, increasing its size slightly and altering its resonant frequency. For an aluminum cavity like ours with Q≈16000 and coefficient of thermal expansion 23 x 10^{-6} m/m-°C[8], a temperature increase of less than 3 °C will expand the cavity by one part in Q (1/16000) and throw a fixed frequency source off resonance.

III. Prospective Error Sources

The section below outlines several prospective error sources in this class of measurement, including due to thermal, RF, magnetic and electrostrictive mechanisms, and where appropriate notes what means are taken to mitigate them or why they are ignored for the time being.

A. Thermal

For any viable thruster the thrusting force should increase with power, motivating testing at as high a power level as practical. However, resonant microwave cavities dissipate their RF power as Ohmic heating caused by induced currents in the resistive cavity walls, so higher RF power directly translates to an increased thermal load in the experimental setup. This thermal load manifests in several ways, including thermal drift and potentially outgassing. We find that thermal drift is a major source of error, while outgassing is not a likely source of concern.

Thermal Drift

A torsional thrust stand is a collection of mechanical assemblies and electronic components, all of which have properties that vary with temperature. The thermal load of the cavity operating at steady state is equal to the RF power (perhaps less some small fraction of the power creating the speculated thrust), and that heat will drive thermal expansion of the stand components, slightly shift the test device's center of gravity, and change the response of electronic components like inclinometers and laser displacement sensors.

An increase from room temperature at about 20 C to an operating temperature near 100 C will expand the approximately 10" long cavity by about .020", shifting the CG by up to .010" or 250 μm. This is significant on a thrust stand where total displacement for 100 μN load is less than 10 μm. Thermal expansion in the wires crossing the torsional pivot bearing and in the arm and base of the thrust stand itself as it heats up due to the DUT thermal load can also drive thermal drift.

To reduce thermal loading and thermal drift at high RF power, we supply RF power from a source outside the vacuum chamber and use a noncontact stripline connector to transfer RF power across a vacuum gap to the resonant cavity. RF power cables for high power application are notoriously stiff and prone to heating, and the power conversion efficiency of RF sources from wall power or DC power is rarely as good as 50%. Keeping the RF source outside the vacuum chamber increases the maximum potential RF power during testing since the RF source can be cooled more easily. The noncontact connector prevents RF cabling from crossing the torsional pivot, eliminating thermal expansion of RF cabling as an error source. It will introduce new risks of RF interference, addressed later.

To further reduce thermal drift, tests are performed at thermal steady state. Resistive heaters mounted to the thrust stand base platform and the DUT provide a steady AC (60Hz) heating power for several hours before testing begins, thermally soaking the experimental setup. Dual PID loops tune the heating currents to maintain the thrust stand base at 50 C and maintain the DUT at a pre-set temperature determined by earlier RF testing at a desired RF power. Due to slight differences in the heating patterns of the resistive vs. RF heating, the temperature of a reference location on the cavity is matched instead of total heating power. Calibration takes place at elevated temperature at steady state, and the heaters are turned off immediately prior to RF testing and restored immediately after RF testing before post-test calibrations. Since the lead wires to the resistive heaters cross the torsional pivot and are also subject to thermal expansion, special care is taken to use flexible, high-strand count wire and to maintain fixed current flow through the lead wires at all times. During RF testing a solid state relay mounted on the torsional arm shorts the heaters to cut the heating power to the cavity while maintaining constant heater current and wire temperature that might affect the arm torsional stiffness.

Finally, to quantify what thermal drift remains, the resonant cavity, thrust stand torsional arm, and thrust stand base are all instrumented with thermocouples to provide some measure of what level of temperature change between AC heating and RF testing occurs.

Outgassing

The small force magnitudes reported in the literature to date, the lack of steady state thermal testing conditions, the presence of non-vacuum rated components including a large dielectric disc inside the cavity, and the lack of reported vacuum chamber operating pressure profiles during thrust recording all raise outgassing as a potential concern. If absorbed water or other volatile species are baked off during testing at elevated temperature, any directionality in the departing species will produce a net thrust force. This would be a real force, in essence a very poor resistojet, and not a drift error, but the force would be short-lived until the volatile species baked off.

To evaluate whether an outgassing event of sufficient magnitude to create a measurable force could have escaped notice in testing to date, consider an operating pressure in the 10^{-6} Torr range giving a typical visible pressure gauge resolution of $\Delta P = 1 \times 10^{-7}$ Torr, with a pumping speed S = 300 L/s comparable to the value for the turbopump used by White. We note the following conversion equations between volumetric flowrates in standard cubic centimeters per minute (sccm), atomic flowrate, and mass flowrate from Goebel (see App. B of Ref. [9]):

$$1 sccm = 4.477962 \times 10^{17} \frac{atoms}{s} = 0.01267 \frac{Torr - L}{s} = 7.43583 \times 10^{-4} M_a \frac{mg}{s}$$

where M_a is the fluid mass in atomic mass units (amu). The gas throughput ΔQ associated with the visible increase ΔP in the chamber pressure with pumping speed S is then

$$\Delta Q = S \Delta P = \left(300 \frac{L}{s} \right) \left(1 \times 10^{-7} Torr \right) = 3 \times 10^{-5} \frac{Torr\, L}{s}$$

which we convert to a volumetric (v-dot) and mass (m-dot) flowrate via the conversions above, assuming water with $M_a = 18$ amu is the typical dominant outgassing species:

$$\dot{v} = \left(3 \times 10^{-5} \frac{Torr\, L}{s} \right) / \left(0.1267 \frac{sccm}{Torr\, L / s} \right) = 0.0024\, sccm$$

$$\dot{m} = \left(0.0024\, sccm \right) / \left(7.43583 \times 10^{-4} \left(18\, amu \right) \right) = 3.17 \times 10^{-5} \frac{mg}{s}$$

Assuming all these particles leave at a temperature of 300 K and form a perfectly collimated beam aligned with the thrust axis with thermal velocity v_{th} gives a thrust T:

$$v_{th} = \sqrt{\frac{kT}{m}} = \sqrt{\frac{\left(1.38 \times 10^{-23} \frac{J}{K} \right) \left(300 K \right)}{\left(18\, amu \right) \left(1.66 \times 10^{-27} \frac{kg}{amu} \right)}} = 372 \frac{m}{s}$$

$$T = \dot{m} v_{th} = \left(3.17 \times 10^{-5} \frac{mg}{s} \right) \left(10^{-6} \frac{kg}{mg} \right) \left(372 \frac{m}{s} \right) = 0.012 \mu N$$

For an outgassing event with a pressure spike of 1×10^{-7} Torr or less, even this conservative value for thrust would be far beneath notice. The effect is linear in pressure, so observed forces of 100 μN due to outgassing would have associated pressure spikes of order 10^{-3} Torr. Neutral outgassing is therefore not a viable explanation for the observed anomalous forces.

Nevertheless, to guard against faulty assumptions above, the chamber pressure is recorded digitally and any variations above the baseline will be noted. If significant pressure spikes are observed, a residual gas analyzer will also be engaged to monitor species from 0-100 amu during all tests, and these traces are also reported.

Finally, to promote rapid evacuation of the resonant cavity at high vacuum, several vent holes are located on the endplates in the null (non-current carrying) locations of the 212 mode excited during this test. These holes double as fastener locations for securing dielectric discs at each end of the cavity. The small holes do not significantly affect the Q of the cavity, and they are far smaller than the resonant wavelength so do not permit RF leakage.

Convective Air Currents

Any atmospheric pressure thrust measurements requiring accuracy in the microNewton range raise concerns that convective air currents caused by DUT heating might appear as spurious thrust forces.[10] The recently test by White was at vacuum,[1] as is this reported test. We do not consider convective wind currents as a major source of error at high vacuum.

B. RF Effects

RF power can do many worrisome things to affect thruster performance measurements, including radiate, generate electromagnetic interference, ionize particles and create plasma, and generate multipactor discharges across gaps. In lieu of a deep dive into specific error mechanisms associated with RF power on a thrust stand, in our initial IV&V we will largely rely on dummy load testing as a gross check that the RF power delivery system is not causing false thrust, and leave investigations into RF interplay with the resonant cavity for future work if merited. Nevertheless, below we discuss plasma production and interference as a spur to discussion.

Plasma Discharges or Ion Production

We largely dismissed a possible warm gas thruster effect during outgassing as an error source given the large gas flow rates and noticeable pressure spikes that would be required to produce ~100 μN force from directed warm neutral flow. However, might the strong fields present in the resonant RF cavity be sufficient to ionize trace gas particles, accelerating a small number of ions to high velocity? This also seems unlikely based on the low background pressures in the chamber, and at present we do not explicitly test for it.

However, assuming this mechanism were viable, one would expect to see a slow decrease in the magnitude of the thrust force as any outgassing species are baked out of the hot cavity and its surroundings. This effect should continue on subsequent test days as the chamber base pressure gradually reduces to ultimate pressure. Conversely one would expect thrust to increase dramatically if background gas were fed into the chamber. If these symptoms occurred one could install a Faraday cup on each side of the cavity to detect any stray ion current.

Interference with other signals

To ensure that RF interference is not causing a spurious effect, we run RF power to a high-power dummy load placed on the torsional arm prior to any cavity testing. The RF noncontacting finger joint is oriented similarly between the dummy and cavity tests, providing an initial check that neither heating nor leakage from the finger joint produce spurious test signals.

In later testing it will be possible to run RF power to the resonant cavity in active and null orientations if merited, all level to horizontal: forward, reverse, and radially inward or outward. Due to the orientation of the finger joint it would be difficult to aim the cavity straight up or down. In later tests if anomalous thrust is observed we may monitor radiated RF power levels using one or a series of drooping-ground plane monopole antennas near the cavity, but during initial testing we will rely on numerical simulations in Altair FEKO that emissions from the cavity and the joint are minimal.

C. Magnetic Tearing or Dipole Coupling

Magnetostatic effects are familiar in Hall thruster testing where “tearing” occurs when strong DC magnetic fields from the DUT couple with magnetic components in the thrust stand to produce operating condition-dependent false thrust readings. There are no applied DC magnetic fields in a resonant microwave cavity, so it is not clear how such a coupling would have occurred in literature reports of thrust in impulse drives, especially since the anomalous thrusting force is associated only with the turn-on of RF power. However, in our experiment the heating currents of several amperes running through the resistive heaters on both the cavity and the thrust stand baseplate will produce magnetic fields, and the heating current through the cavity will turn off each time the RF power turns on, and vice versa. There is a potential for magnetic effects there.

To minimize the magnetic field generated by the heaters we use alternating current (60 Hz), so dipole coupling should wash out in the ~1 Hz time-averaged thrust displacement readings. In addition to this mitigation technique, we can also bound the maximum thrust error by measuring the swing in readings induced by running DC current of opposite polarities through the cavity heaters.

The cavity, thrust stand and immediate environment are also almost entirely constructed of nonmagnetic materials, primarily aluminum, 316 stainless steel and various plastic components. The exceptions are the small permanent magnets in the damper assembly and some magnetic steel in the large optical table supporting vibration isolation stage and thrust stand, approximately 18" below the DUT.

D. Electrostriction

An outstanding puzzle for the whole class of proposed impulse drives is how harmonic fields are supposed to generate a net force. Since the electromagnetic fields everywhere in the cavity are sinusoidal, they point in equal and opposite directions over each RF cycle – therefore, shouldn't any "pushing" anywhere in the system balance out to zero?

One possible rectifying phenomenon is electrostriction. Electrostriction is the general material property that nonconductors expand when placed in an electric field, as ions in the crystal lattice respond to the applied field and induce a slight strain. The effect is rectifying because materials only undergo expansion from the rest state, so regardless of the electric field direction E the material gets longer. This effect is proportional to E^2. Most materials experience only miniscule strains, and since the phenomenon is mechanical due to physical displacement of ions in the crystal lattice, it generally is restricted to exciting frequencies <100 kHz. However, previous work at NRL has shown that electrostriction can be induced in materials by exciting frequencies in the GHz range, provided a second nearby signal produces a beat frequency in the appropriate kHz range.[11] In the work cited, this phenomena was leveraged for microwave signal detection in a fiber optic electrostrictive sensor by exciting a locally applied 1-20 GHz signal with remotely sensed microwave signals.

In our experimental configuration, one potential source for a nearby frequency source is from sidebands in the applied microwave signal to the cavity. Both the synthesizer and amplifier are in principle capable of generating low-amplitude sidebands within 100 kHz of the main driving frequency, and such sidebands have been noted in passing though not yet specifically quantified in frequency or amplitude. Moreover, these sidebands will also resonate if they are within the resonant bandwidth of the cavity, which spans about +/-50 kHz for our cavity with Q≈16000 at 1.86 GHz.

If this mechanism is found to be plausible after further investigation, a reasonable experimental test would be observe whether a cylindrical resonant cavity filled almost completely with a dielectric insert, but secured only to one endcap of the cavity, still produces an anomalous force. Such a configuration ought to produce no or minimal anomalous force under any propulsive theory by symmetry arguments, so any detected force could be attributed to an electrostrictive effect. An added bonus is that a cylindrical configuration almost filled with a dielectric would be analytically tractable to a close approximation. Alternately, a fiber optic sensor like the one reported in Ref. [11] could be inserted into a proposed thruster cavity dielectric as a sensitive, nonintrusive strain gauge to directly verify an electrostrictive response.

IV. Experimental Setup

A. Vacuum Facility

All testing reported in this paper takes place in the South Chamber, a 2.3m tall by 2 m diameter upright cylindrical stainless steel chamber. The chamber is mounted vertically and suspended about 3 meters in the air, with the bottom endcap raised and lowered by a hydraulic lift. The thrust stand is fixed to the endcap and brought to ground level for experimental access.

South Chamber is brought to rough vacuum by a Leybold WH2500 blower and SV-630B roughing pump with combined pumping speed 1530 CFM, and maintained at high vacuum by a NRC 48" diffusion pump with nominal

pumping speed 100,000 L/s on air. Due to conductance losses through internal shrouds for thermal vacuum cycle testing, the effective pumping speed of the diffusion pump is reduced to an effective speed of about 20,000 L/s, giving a typical base pressure in the low to mid 10^{-6} Torr range after 24 hours at high vacuum. High vacuum pressure is monitored using a Bayard-Alpert type hot ion gauge.

B. Torsional Stand

The torsional thrust stand used for this work was manufactured by Busek Co. for NRL and is described in much greater detail by Williams.[12] The base and free-swinging arm of the stand are joined by two stainless steel Riverhawk flexural pivots. The stand and arm are each made of dip-brazed aluminum to relieve thermal stresses and have a chromate conversion coating to prevent static charging. The arm is 48 cm long with two 7.5 cm square mounting platforms at each end. The moment arm from the torsional axis through the center of the mounting platform where the device under test (DUT) is placed is 20 cm. The DUT is alone at one end of the arm, while the other end houses the balance mass to counteract the gravitational load of the DUT on the torsional pivots, the mirror for the optical displacement sensor, and one of the two metal discs used as a capacitive force generator (CFG). The entire stand is mounted to a 24" square x ½" thick black anodized aluminum optical breadboard.

The optical displacement sensor (ODS) is a Philtec model D63. The sensor has an accuracy of 25 nm at a distance of approximately 1 mm from the mirror, in the so-called "far side" of the instrument response curve. A nominal spring constant for the system is of order 15-20 μN/μm. Optical signals from the ODS are passed through two fiber optic cables to measurement electronics outside the vacuum chamber.

The capacitive force generator (CFG) calibrates the displacement response of the ODS to a known applied electrostatic force. Two conducting discs, one attached to the torsional arm and the other mounted to the optical breadboard, are swept through a series of gap spacings and the capacitance of the two discs is measured at each gap by a BK Precision 889B LCR meter. The force between the two plates is a known function of the plate capacitance, applied voltage, and gap distance, so by measuring the capacitance and monitoring the gap spacing the voltage can be swept to generate a range of applied forces to calibrate the ODS response. The capacitive plates are shorted together when not in use to prevent inadvertent bias.

Oscillations induced by ambient environmental vibration and shocks are damped by inducing eddy currents in a 2" x 3" x 1/8" copper plate suspended from the balance end of the torsional arm. Two ¾" square x 1/8" thick neodymium magnets are mounted on a motorized stage oriented parallel with the torsional arm and positioned close to the copper damping plate to excite eddy currents when the plate moves back and forth in front of the permanent magnets. The separation between the magnets and the copper plate is reduced until the arm oscillation is slightly underdamped.

The 24" square black anodized aluminum optical breadboard is thermally stabilized during testing at 50 C using a LabView software PID loop running at 1 Hz. The process temperature is read from a K-type thermocouple mounted to the thrust stand base by a Measurement Computing E-TC multichannel thermocouple reader. The PID output is used to compute a 60 Hz sine wave RMS voltage output on an Agilent 33512B waveform generator, which in turn drives the analog input of a Kepco BOP 36-12M bipolar amplifier in current control mode to produce a 60 Hz AC current through a set of sixteen parallel Minco HK5249 53 Ω polyimide Thermofoil heaters distributed across the breadboard, for an effective 3.3 Ω resistance.

To balance the stand, the DUT mass is measured to 0.1g accuracy, and an approximately equal mass of fine tungsten carbide powder in a glass jar is placed on the balance end of the arm. Tungsten carbide's high density makes it a very effective ballast mass in a small volume, and the powder form permits easy adjustment to match varied weight conditions.

C. Resonant Cavity

Mechanical Design

The DUT cavity closely replicates the internal geometry (length, diameter and taper) reported by White with an independent mechanical, thermal and RF power feed design. This replica cavity (see Figure 1 and Figure 2) is of two piece aluminum construction, with a .001" thick copper plating applied to improve surface conductivity. Sixty-eight 8-32 fasteners and thirty-four plate nuts uniformly clamp the lid shut. The base piece of the cavity has internal length

9", large diameter 11", small diameter 6.25" and an additional .093" radius fillet at the small end to improve machinability from a single piece of aluminum. The internal surface of the lid has an 11" diameter, .025" deep recess to permit focused lapping of the lid clamping surface, bringing the total cavity internal length to 9.025". This recess has a .020" radius fillet. The total mass of the assembled cavity is approximately 3 kg.

A second, dummy resonant cavity was also fabricated to support benchtop testing. This dummy cavity is a squat aluminum cylinder used as a testbed for the resonance tuning closed loop feedback circuit. It also uses a two piece lid-and-base construction, with internal diameter D = 3.688" and height H = ½*D = 1.844". A "candlestick" style SMA connector mounted off center on the lid excites the cavity at a fundamental frequency of 2.45 GHz with a quality factor of approximately 5000. Twenty ¼-20 fasteners provide strong uniform clamping pressure to secure the lid to the base. Aside from light lapping of the interface between lid and base, no post-machining of the cavity was performed after CNC milling.

Thermal Design

Initial tests of the bare cavity confirmed that the low emissivity of the copper plating drove excessive heating. This motivated application of a high-emissivity coating in preparation for thrust stand testing. Radiated power varies linearly with emissivity so increasing the device emissivity directly increases the maximum permissible operating power given operating temperature limits. The high emissivity coating also enables more rapid thermal equilibration, though this still takes a few hours at vacuum.

Our self-imposed requirement to test at thermal steady state and desire to decouple RF-induced effects from thermal effects also motivate the use auxiliary resistive heaters on the cavity. Several polyimide test heaters (Minco models HK5422 35 Ω and HK5334 38 Ω) are applied to the cavity walls and lid to permit cavity heating independent of RF power. Eight parallel 35 Ω heaters on the lid are wired in series to sixteen parallel 38 Ω heaters on the cavity walls to create an effective 6.7Ω resistor covering much of the outer cavity surface. To prevent magnetic tearing due to dipole coupling the heaters run off 60 Hz AC power in a temperature-stabilized PID mode identical to the baseplate heating discussed earlier. The acrylic adhesive on the heater sets our test temperature ceiling of 100 °C. Future testing at higher temperatures up to 200 °C and thus higher power as well would be possible with clamped heaters in place of acrylic adhesive heaters.

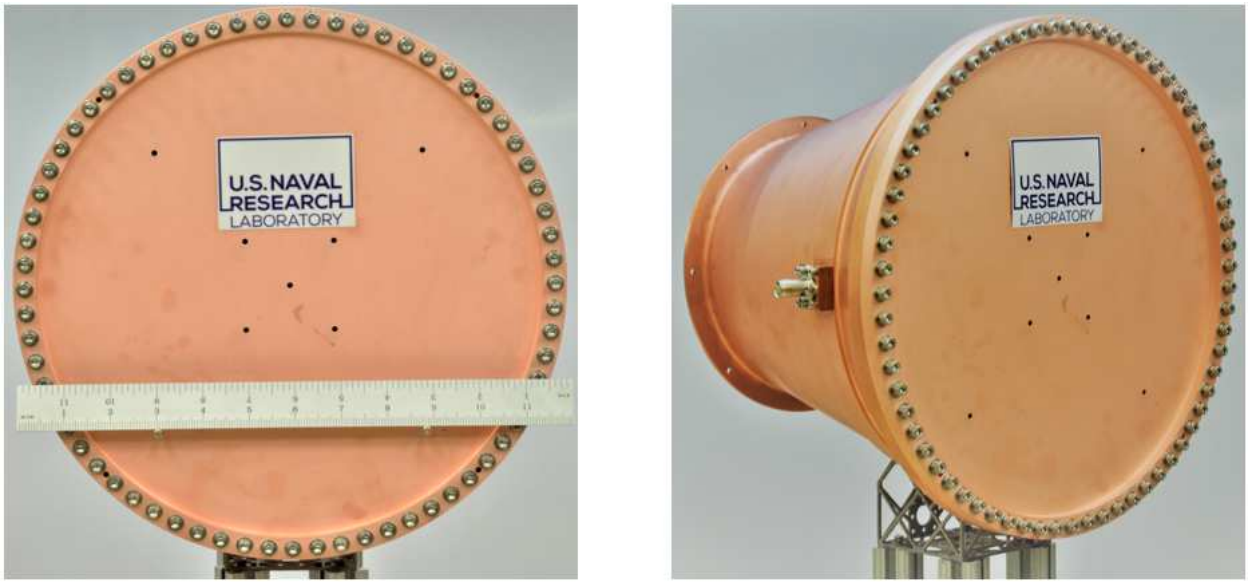

Figure 1: NRL's replica cavity reproduces the relevant internal resonant geometry of the NASA JSC design with independent mechanical, thermal and RF power feed design.

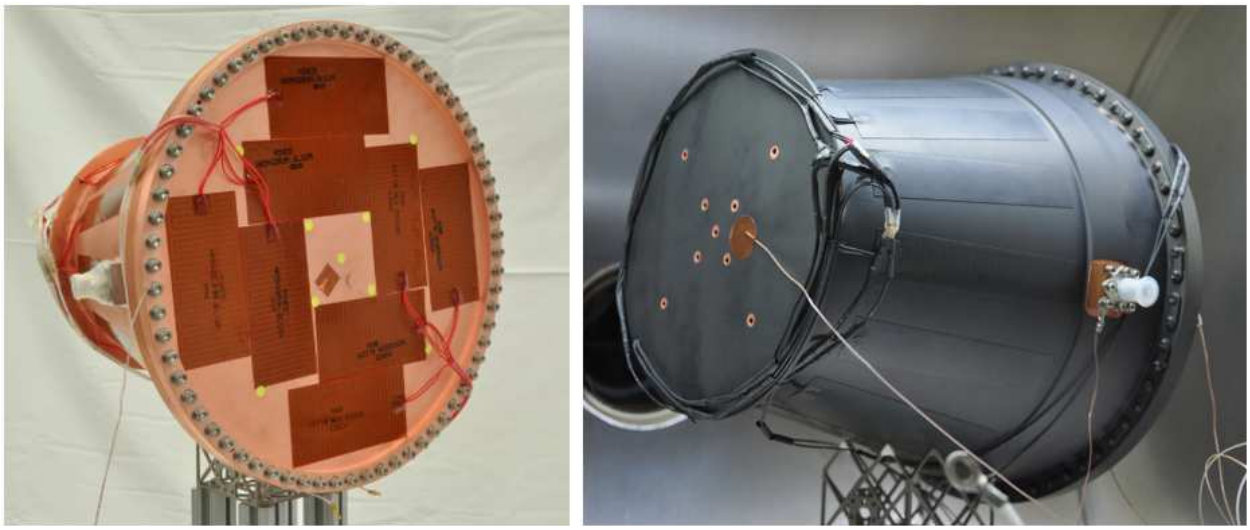

Figure **2**: Cavity with **resistive h**eaters**, before (left) and after (right) h**igh-**e**missivity **c**oating

Polymer Insert

An apparently crucial contribution to the anomalous force reported by White et. al. is provided by a high density polyethylene (HDPE) disc approximately 6" diameter x 2" thick inserted in the small end of the cavity. While no published data comparing force production with and without an insert is available, and the mechanism by which this disc contributes to the thrust has not yet been fully described, we replicate it in our planned test configuration as well. We plan to run initial cavity thrust stand testing without the insert before running a second set of tests with the insert installed. Assuming the cavity without the critical insert produces no or negligible anomalous thrust, this will be an additional level of control testing.

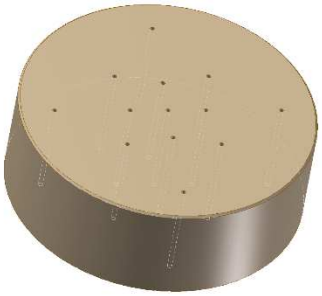

Figure 3: Polymer insert for NRL replica cavity (CAD image)

The NRL insert is a cut from a rod of extruded HDPE into a disc 15.6 cm diameter x 5.4 cm thick. A (presumably) minor difference from the NASA insert is the inclusion of several thru holes .089" in diameter aligned with the vent holes on the lid and base of our replica cavity. These holes are tapped to permit attachment of the insert to either end of the replica cavity as desired using alumina ceramic bolts. Thru holes instead of tapped holes were chosen to remove the possibility of trapped gas volumes in blind holes in the insert, and to facilitate any initial volatile outgassing of the material during vacuum bakeout. One other minor difference is a 1mm chamfer on the bottom edge of the insert to allow a flush fit in the small end of the replica cavity, which has a small fillet.

RF Design

Initial rough RF design and mode calculations were performed semi-analytically by numerically solving the Maxwell equation boundary conditions for the resonant TE and TM modes in a cavity replicating the NASA internal dimensions but with a spherical endcap geometry. This provided an approximate roadmap to which modes to expect at which frequencies in the flat endcap geometry of the frustum replica cavity.

Subsequent detailed RF design work including loop antenna placement, antenna sizing and RF transmission joint design was performed using Altair FEKO. Mode identification in FEKO was performed using slices at various axial and azimuthal locations to view electric and magnetic field strengths, and matched to the nearby predicted modes of the spherical endcap cavity.

The cavity RF feed is a TNC connector mounted 6.75" axially from the small end of the cavity. A small coupling loop protrudes into the cavity, mounted normal to the cavity wall. One lead of the loop is soldered to the center conductor of the connector while the other end is screwed into a copper adapter block mating the connector to the cavity. The connector, copper adapter and cavity are mechanically secured by 4-40 screws. The cavity is tuned by adjusting the diameter of the coupling loop; the loop is not rotated within the cavity.

D. Dummy Load

We use a high power RF dummy load (Bird 250-CT-FT, 50 Ω, 250 W), modified significantly to operate in a vacuum environment, mounted to an aluminum block heatsink with black anodized aluminum radiator fins. The dummy load uses similar Minco resistive heaters as the cavity and is approximately the same height so it can use the same noncontact finger joint for RF power. The all-aluminum construction is designed to maximize conductive heat transfer, and the black anodized fins are sized to radiate approximately 100 W at 100 °C so that the load can run at approximately the same power levels and temperatures as the cavity.

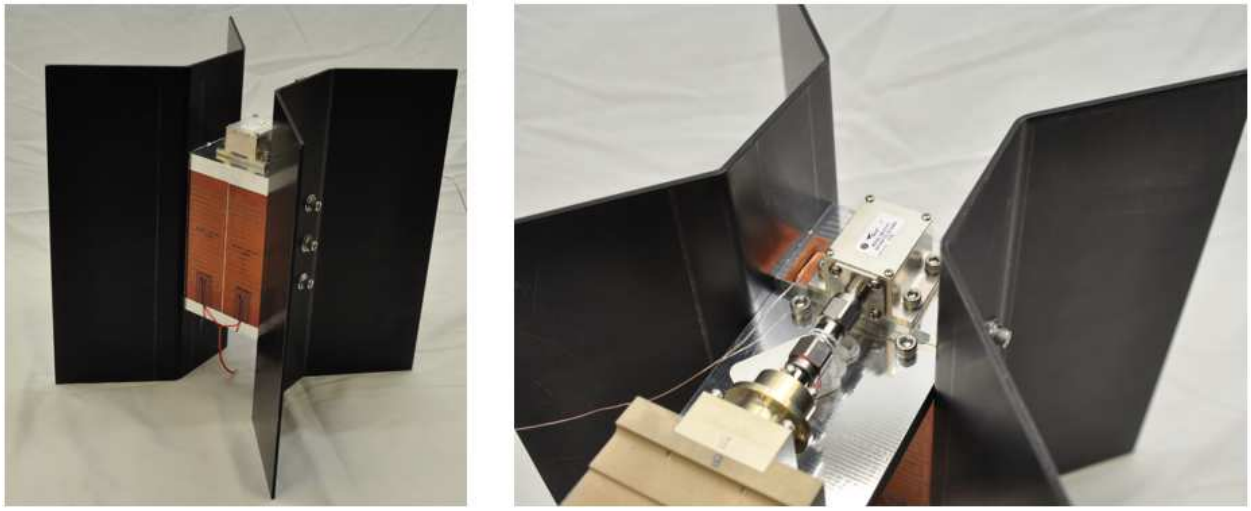

Figure 4: RF **dummy load with resistive heaters and radiator fins**

E. RF Power Generation and Transmission

The simplest experimental knob to turn to increase the SNR is to increase driving RF power, as for any claimed thruster the thrust should increase with power. White reports thrust / power of order 1-2 microNewtons per watt (μN/W) at 80 W total forward RF power. The challenge of testing at several 10s-100s W in the few GHz frequency range is minimizing the thermal load to the torsional stand. We approach this problem by performing RF signal synthesis and amplification outside the vacuum chamber and routing power approximately 15 feet from the amplifier through a vacuum feedthrough and onto the thrust stand, using a custom noncontacting power transmission joint to cross the torsional pivot from the thrust stand base to the torsional arm.

Wall Power to Thrust Stand: RF Generation, Amplification and Vacuum Feedthrough

An Agilent N5171B 9 kHz – 3 GHz signal generator drives an approximately 2 GHz signal to an IFI S251 0.8 – 2.5 GHz 150 W solid state microwave power amplifier. The high power signal passes through a Narda 3022 20 dB directional coupler to a ~8' Andrew LDF4-50A heliax coaxial cable and into the vacuum chamber through a Radiall R143.753.000 TNC hermetic bulkhead feedthrough. Inside the vacuum chamber, power continues through two flexible Micro-Coax UFB311A cables with high-power TNC connectors, the first 52" long and the second 26" long, joined through another identical Radiall bulkhead feedthrough inside the chamber. The shorter 26" cable terminates at the stationary side of the noncontact finger joint, discussed below. All cables were chosen from on-hand materials for their relatively low loss, and the use of two cables at vacuum was to permit intermediate strain relief and thermal heatsinking for the long, relatively stiff cables. The longer 52" vacuum cable uses additional heatsinking through copper straps near the cable midpoint.

At atmosphere, both the forward and reflected power outputs of the Narda directional coupler go to separate Narda 3372A-4 4-port power dividers for direct visual monitoring, telemetry, and feedback control. Forward power spectra, as well as reverse second harmonic and reverse close-in noise floor (both for multipactor detection) are visually monitored on two Agilent E4443A spectrum analyzers. The forward and reflected power telemetry are recorded from two Agilent E4418B power meters with Agilent 8481A power sensors. An analog 0-100 mV reflected power signal is produced by a HP 423B Schottky diode detector for closed loop frequency feedback control.

Thrust Stand to DUT: Noncontact RF Power Transmission

RF power transmission from the stationary thrust stand base to the freely swinging torsional arm is accomplished through a noncontact "finger joint", so named for its side-on appearance of interlocking fingers. The design is based on a stripline geometry, which takes advantage of the lack of azimuthal currents in a coaxial cable or waveguide to split the shield conductor in half and flatten it to a rectangular geometry with length and width adjusted to maintain a 50-ohm impedance. In the finger joint the center conductor and ground planes are both split into axially overlapping sections that are nominally λ/4 in length at the cavity operating frequency; other portions of the geometry are chosen to maximize the capacitance to significantly extend the lower frequency end of its operating range. The result is a joint that has a relatively large bandwidth about its nominal design frequency to permit testing of multiple resonant modes in the future if desired.

Figure 5: Left, a cross-section of a typical round coaxial waveguide compared to the rectangular cross section of a stripline; right, a side view of a conceptual finger joint showing the splitting of the stripline pieces into overlapping fingers.

Figure 6: Side view of finger joint showing overlapping ground and center conductor plane to allow operation over a range from 0.7 - 2.5 GHz

V.Preliminary Thermal and Resonance Results

No thrust stand performance measurements have been performed on the thrust stand. However, initial tests of thermal response, frequency feedback control, temperature stabilization, and finger joint performance have been completed. These are discussed below.

F. Bare Cavity RF Heating with Cable

Initial RF resonant heating of the bare copper cavity, shown above in Figure 1 and below in Figure 7, demonstrated good ability to stay on resonance over several hours using the closed loop frequency feedback tuning, even during rapid temperature changes. The tests also indicated that the cavity as fabricated would get extremely hot at relatively low input power due to its very low emissivity. This low emissivity created a near isothermal cavity, as conduction was far favored over radiation all over the cavity, and it caused very long thermal equilibration times. This motivated the high emissivity coating shown in the next section. The RF cable did not see high temperatures during this test, peaking at less than 40 °C.

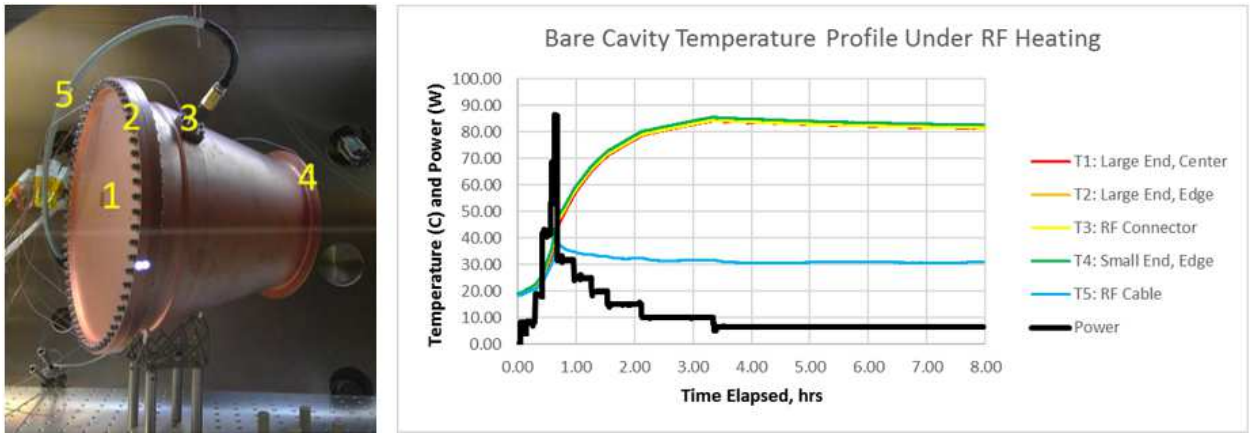

Figure 7: Left, the bare copper cavity mounted in the PTF with thermcouple locations shown; right, the temperature profile over 8 hours to arrive at an accelerated thermal equilibrium

A. Black Cavity DC Heating with Cable

After coating the cavity for higher emissivity, the available operating power range expanded dramatically. We were able to operate at nearly 85 W while maintaining peak temperatures under 100 °C. This test used direct current (DC) resistive heating, and is important as a comparison with the next section using RF heating. There is an approximately 30 C temperature difference between the center of the large end of the cavity and the center of the small end. Note that thermocouples T4 and T5 are in different locations during this test. Thermocouple T4 moved from the edge of the cavity small end to the center of the cavity small end, and T5 moved from the RF cable (not present in this test) to the solid state relay shown at bottom left in Figure 8. The relay saw temperatures peaking at about 30 C, with slightly higher temperatures starting at about 2 hours when it was actuated to short the cavity resistors while maintaining constant heating current.

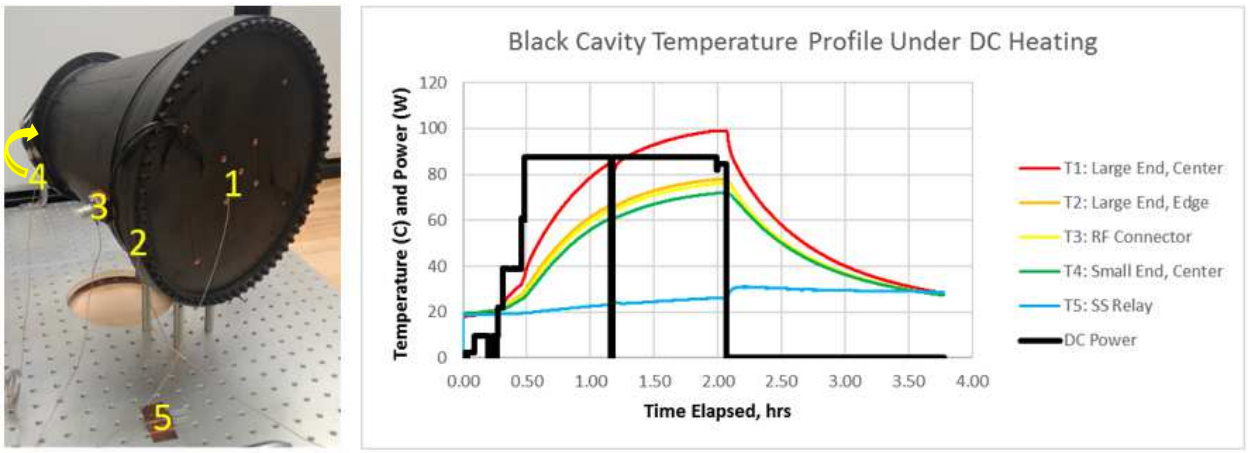

Figure 8: Left, the black cavity with thermocouple locations shown; right, the temperature profile over 4 hours under DC heating. Note that thermocouples T4 and T5 are in new locations.

B. Black Cavity RF Heating with Cable

The RF testing of the black cavity showed a wider spread of temperatures than in the initial bare cavity case, but only about 15 °C from one end of the cavity to the other, less than produced by the resistive heating. This suggests that the eddy currents in the cavity are spread more uniformly than the resistor placement can reproduce. Figure 9 is for approximately the same total power as Figure 8, with a slightly lower peak temperature. Notably at this near-full power condition the RF cable is still only at about 65 °C.

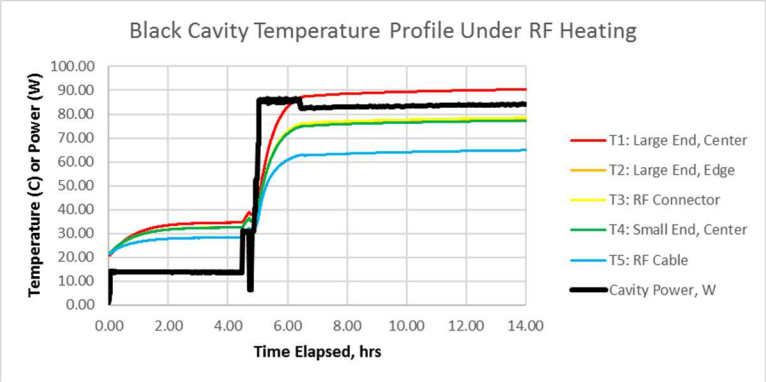

Figure 9: Heating profile under resonant RF power for the black cavity, showing steady operation just over 90 C at about 85 W power.

C. Dummy Load RF Heating with Finger Joint

The final test to date validated the feasibility of aligning the noncontact finger joint and maintaining alignment at high power in spite of thermal expansion. This test took place at 100 W power and monitored temperature of the aluminum block immediately adjacent to the dummy load, as well as on the RF cable as before. Because of this placement, the thermocouple will often register an initial spike in temperature at a new power before the heat conducts sufficiently to the radiator fins to enable a cooler steady state temperature. As a result, the profile in Figure 10 has a rapid ramp to just over 100 C at only 50 W applied power, then after a pause was able to accommodate a full 100 W power input with temperature under 100 C. The total return loss throughout this test was about 23 dB, much of which is due to the dummy load itself rather than the finger joint.

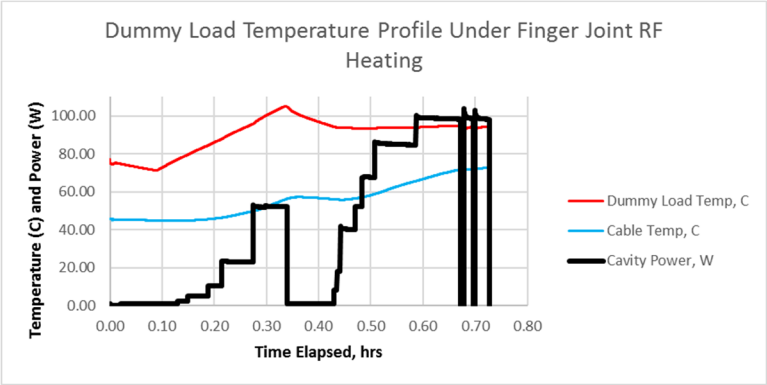

Figure 10: Excerpt of a dummy load heating profile. The radiator fins take a while to heat up and wick heat from the load, so the load was rapidly heated to near-operating temperature at about 50% power and allowed to partially equilibrate before going to full power.

VI. Conclusions

This paper has presented the basic design drivers and experimental pitfalls for a high-fidelity impulse drive test, and outlined initial risk reduction results of a Naval Research Laboratory effort to independently validate and verify (IV&V) the anomalous thrust production reported by White et. al of NASA JSC in a resonant tapered microwave cavity. We have defined an impulse drive as any one of several recently proposed devices that claim to produce thrust without observable reaction mass, in apparent violation of the conservation of momentum. Our default assumption is that any observed thrust is most likely due to experimental error, but the above published results in a peer-reviewed venue compel us to perform IV&V as due diligence to either confirm the results or identify the error.

We have independently designed a replica cavity test article and validated its thermal response to both AC and RF heating. We have also developed a noncontact RF power transmission technique called a finger joint and demonstrated successful power deposition to a dummy load in vacuum on a stationary platform using the finger joint. After reviewing several error mechanisms that can contribute to false readings of thrust, we identify thermal drift and potentially electrostrictive effects as the most promising error candidates.

In the near future we expect to begin vacuum thrust stand testing of the dummy load and finger joint to identify and account for spurious force readings due to thermal drift, RF effects, or both, and to prepare for cavity thrust stand testing with and without a polymer insert. We will test without the polymer insert first, anticipating this as an additional control test which is not expected to produce any anomalous force, and follow with tests of the cavity with insert. All tests will be conducted at thermal steady state or as close to it as practical.

VII. Acknowledgments

The authors wish to gratefully acknowledge Dr. Harold White of NASA Johnson Space Center for many helpful discussions of his test setup, methods and apparatus.

References

[1] H. White *et al.*, "Measurement of Impulsive Thrust from a Closed Radio-Frequency Cavity in Vacuum," *J. Propuls. Power*, vol. 0, no. 0, pp. 1–12, 2016.
[2] R. Shawyer, "Second generation EmDrive propulsion applied to SSTO launcher and interstellar probe," *Acta Astronaut.*, vol. 116, pp. 166–174, Nov. 2015.
[3] H. Fearn, N. van Rossum, K. Wanser, and J. F. Woodward, "Theory of a Mach Effect Thruster II," *J. Mod. Phys.*, vol. 06, no. 13, p. 1868, Oct. 2015.
[4] T. Quinn, H. Parks, C. Speake, and R. Davis, "Improved Determination of G Using Two Methods," *Phys. Rev. Lett.*, vol. 111, no. 10, p. 101102, Sep. 2013.
[5] T. Quinn, C. Speake, H. Parks, and R. Davis, "The BIPM measurements of the Newtonian constant of gravitation, G," *Phil Trans R Soc A*, vol. 372, no. 2026, p. 20140032, Oct. 2014.
[6] L. T. Williams and M. L. R. Walker, "Thrust Measurements of a Radio Frequency Plasma Source," *J. Propuls. Power*, vol. 29, no. 3, pp. 520–527, 2013.
[7] A. Shabshelowitz and A. D. Gallimore, "Performance and Probe Measurements of a Radio-Frequency Plasma Thruster," *J. Propuls. Power*, vol. 29, no. 4, pp. 919–929, 2013.
[8] *CRC Handbook of Chemistry and Physics*, 92nd ed. Boca Raton, FL: CRC Press, 2012.
[9] D. M. Goebel and I. Katz, *Fundamentals of Electric Propulsion.* John Wiley and Sons, 2008.
[10] D. Brady, H. G. White, P. March, J. T. Lawrence, and F. J. Davies, "Anomalous Thrust Production from an RF Test Device Measured on a Low-Thrust Torsion Pendulum," presented at the AIAA/ASME/SAE/ASEE Joint Propulsion Conference, 28-30 Jul. 2014, United States, 2014.
[11] S. T. Vohra and L. Fabiny, "Mixing and detection of microwave signals in fibre-optic electrostrictive sensor," *Electron. Lett.*, vol. 30, no. 5, pp. 444–445, Mar. 1994.
[12] L. T. Williams, M. S. McDonald, and M. F. Osborn, "Performance and Vibration Characterization of a Low-Thrust Torsional Thrust Balance," in *35th International Electric Propulsion Conference*, Atlanta, GA USA, 2017.